Inorganic Chemistry

Article

pubs.acs.org/IC

# Direct Measure of Metal−Ligand Bonding Replacing the Tolman Electronic Parameter

Dani Setiawan, Robert Kalescky, Elfi Kraka, and Dieter Cremer*

Computational and Theoretical Chemistry Group (CATCO), Department of Chemistry, Southern Methodist University, 3215 Daniel Avenue, Dallas, Texas 75275-0314, United States

Supporting Information

**ABSTRACT:** The Tolman electronic parameter (TEP) derived from the $A_1$-symmetrical CO stretching frequency of nickel-tricarbonyl complexes L−Ni(CO)$_3$ with varying ligands L is misleading as (i) it is not based on a mode decoupled CO stretching frequency and (ii) a generally applicable and quantitatively correct or at least qualitatively reasonable relationship between the TEP and the metal−ligand bond strength does not exist. This is shown for a set of 181 nickel-tricarbonyl complexes using both experimental and calculated TEP values. Even the use of mode−mode decoupled CO stretching frequencies (L(ocal)TEPs) does not lead to a reliable description of the metal−ligand bond strength. This is obtained by introducing a new electronic parameter that is directly based on the metal−ligand local stretching force constant. For the test set of 181 nickel complexes, a direct metal−ligand electronic parameter (MLEP) in the form of a bond strength order is derived, which reveals that phosphines and related ligands (amines, arsines, stibines, bismuthines) are bonded to Ni both by $\sigma$-donation and $\pi$-back-donation. The strongest Ni−L bonds are identified for carbenes and cationic ligands. The new MLEP quantitatively assesses electronic and steric factors.

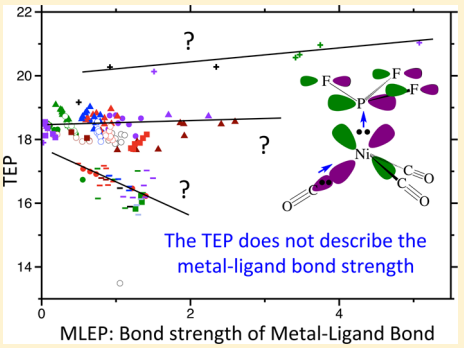


## 1. INTRODUCTION

Experimentalists describe the strength of metal−ligand bonding by using the Tolman electronic parameter (TEP).[1,2] The TEP is based on the $A_1$-symmetrical CO stretching frequency of nickel tricarbonyl phosphine complexes of the type L−Ni(CO)$_3$ with L = R$_3$P. Since this vibrational frequency is separated from other frequencies in the infrared spectrum, it can be easily measured. The carbonyl ligand is sensitive to the electronic structure at the metal atom. Any ligand that increases the electron density at the metal atom converts the latter to a potential nucleophile that shifts via $\pi$-back-donation negative charge to the carbonyl, which accepts charge in its low-lying $\pi^*$(CO) orbital. Accordingly, the CO bond is weakened, and the value of the CO stretching frequency is lowered. This decrease can directly be registered in the infrared spectrum and gives the TEP its importance as an indirect descriptor for the metal−ligand (ML) bond strength. Even in the 1960s, several authors pointed out the relationship between the ML bond strength and the value of the CO stretching frequency,[3−6] but it was Tolman who systematized this approach in two ways: (i) deriving the TEP from the $A_1$ CO stretching frequency in $C_{3v}$-symmetrical carbonyl complexes and (ii) using nickel-phosphine complexes because these ligands possess a distinct electronic and steric tunability, seldom participate directly in the reactions of a transition metal complex, and as such can be used to modulate the electronic properties of the adjoint metal center.[7] Typical TEP values for phosphines range from 2111 cm$^{-1}$ for PF$_3$ (weak electron donor) to 2056 cm$^{-1}$ for P(t-butyl)$_3$ (strong electron donor).[1,2,8]

The use of the CO stretching frequency as a quantitative indicator for ML bonding has been realized in literally hundreds of investigations focusing on transition metal complexes. Only some of them can be mentioned here. TEP values were derived via infrared spectroscopy for carbonyl complexes of vanadium,[4] chromium,[9−12] molybdenum,[4,6,13−16] tungsten,[4,9,16−19] rhenium,[20] iron,[21−28] ruthenium,[29] rhodium,[30−39] iridium,[30−32,38−41] nickel,[42,43] gold,[44−46] and zinc.[47]

The wide interest in obtaining reliable TEP values caused computational chemists to determine CO stretching frequencies of carbonyl-metal complexes in the harmonic approximation for molecules in the gas phase and to use them as a computational electronic parameter (CEP) for the description of ML bonding.[48] Most of the computational investigations suggest that CEPs obtained for Ni, Ir, or Ru complexes correlate well with the experimental TEPs[49−54] provided DFT functionals, which are suitable for metal complexes, are applied.[51,55,56] CEPs were also calculated for CO adsorbed by Ni−Au clusters.[57] In some cases, CEP values based on semiempirical calculations were published for LMo(CO)$_5$, LW(CO)$_5$, and CpRh(CO)(L) complexes,[58] or rhodium Vaska-type complexes[59] where results depend on the parametrization of the method in question. Several review articles summarized the experimental and theoretical work in this field.[60−62]

**Received:** November 24, 2015
**Published:** February 22, 2016





DOI: 10.1021/acs.inorgchem.5b02711
Inorg. Chem. 2016, 55, 2332−2344

A prominent example for the increasing popularity of the TEP is its application to transition metal complexes containing as a ligand an N-heterocyclic carbene (NHC).[63−66] In recent reviews on NHC compounds, Nelson and Nolan[32] and Dröge and Glorius[30,31] pointed out the widespread and preferred use of the TEP as a tool for experimentalists who investigate the electronic properties of metal-NHC complexes. For the purpose of studying the bonding properties of NHC ligands, usually the corresponding *cis*-[$MCl(CO)_2(NHC)$, M = Rh, Ir] model complexes are synthesized because of the toxicity of the corresponding $Ni(CO)_3(NHC)$] complexes.[30−32,67] Using linear regression schemes proposed by Dröge and Glorius,[31] TEP values obtained from different metal complexes can be correlated. This has led to a large compilation of TEP data for hundreds of NHC ligands, all using the same TEP scale. TEP values for NHCs generally stretch from 2030 $cm^{-1}$ for electron rich NHCs to 2060 $cm^{-1}$ for electron poor NHCs.[30−32] This seems to be a small range of TEP values considering the large variety and complexity of NHC compounds as given by the following representative list: (i) NHCs with extended polyaromatic substituents;[40] (ii) planar chiral imidazopyridinium based NHCs, which can function as Lewis acids and ligands for transition metal complexes;[21] (iii) spiro-fused six-membered NHCs;[68] (iv) polycyclic NHCs featuring a fused dibenz[*a*,*c*]phenazine moiety;[41] (v) nanosized Janus bis-NHC ligands based on a quinoxalinophenanthrophenazine core;[43] (vi) NHCs with O-functionalized triazole backbones;[69] and (vii) cyclic alkyl aminocarbenes as strongly donating ligands at the lower end of the NHC-TEP scale.[29]

As a consequence of the widespread use of the TEP, there are more and more attempts to relate it to or complement it by other measured or calculated properties of the transition metal complex in question. Tolman himself realized that the bulkiness of a ligand can outweigh electronic factors, which was the reason why he introduced the cone angle $\theta$ as a measure for the steric requirements of the ligand.[1,2] The Lever electronic parameter (LEP) is based on the ratio of the redox potentials of closely related complexes such as those of Ru(III) and Ru(II), which can be electrochemically determined[70,71] and which can be set into relationship to the TEP.[48] It has been disputed whether the molecular electrostatic potential can be used to derive the CO stretching frequencies of transition metal carbonyl complexes.[72,73] Alyea and co-workers[74] suggested ways of differentiating between $\sigma$ and $\pi$ effects influencing the CO stretching frequencies by referring to thermochemical data such as $pK_a$ values. Giering[73] combined electronic and steric effects to what he coined the *Quantitative Analysis of Ligand Effects* (QALE) model. Coll and co-workers introduced an average local ionization energy $I(\mathbf{r})$ that, if integrated over the van der Waals surface of L, can be set into relationship to the TEP and Tolman's cone angle as was demonstrated for phosphines and phosphites. However, this approach turned out to be only reliable for ligands with high polarizability.[75] Recently, it has been suggested to characterize NHC−metal bonding via their selenium adducts by measuring $^{77}Se$ NMR chemical shifts and $^{77}Se-^{13}C$ spin,spin coupling constants rather than relying on the TEP.[76]

Despite the large number of seemingly successful applications of the TEP to describe ML bonding, there have been scattered critical comments on the usefulness, applicability, and reliability of the TEP and the associated Tolman cone angle.[20,44,45,55,76−83] In this connection, a rigorous analysis of the TEP was published by Kalescky and co-workers,[56] who questioned one of the basic assumptions made by Tolman to derive a useful electronic parameter. He assumed that the $A_1$-symmetrical CO stretching mode is *free of any coupling with other stretching or bending modes* and thereby provides a direct measure of the electronic effects determining the metal−ligand bond strength. Kalescky and co-workers demonstrated for a limited set of $L-Ni(CO)_3$ complexes that there is a significant amount of coupling, which contaminates any measured or calculated TEP value.[56] Therefore, these authors urged researchers to use a decoupled (local) CO stretching frequency as a local TEP (LTEP), which can reliably describe the electronic situation of the complex. Since this investigation was limited with regard to the number of ligands investigated and because of the fact that sterically demanding ligands were largely excluded, the current work takes a second, more systematic step to scrutinize the usefulness of the TEP and to provide a common platform for the criticism on the TEP raised by other authors in the recent literature.[20,44,45,55,76−83]

For this purpose, 181 $L-Ni(CO)_3$ complexes including a large variety of ligands L with both normal or critical electronic and steric properties are investigated. The basic shortcomings of the TEP will be revealed on a quantitative basis where we will make ample use of the local vibrational mode approach of Konkoli and Cremer.[84] At the end of our analysis, the TEP will be revealed as a misleading parameter, which provides only in a few ideal cases a reliable insight into ML bonding and thereby into the electronic structure of the transition metal complex in question. Otherwise, it has to be replaced by a new and direct *metal−ligand electronic parameter* (MLEP), which provides a quantitative measure of the strength of the ML bond in a way that is urgently needed for a reliable description of transition metal complexes in synthesis and catalysis.

The results of this work are presented in the following way. In section 2, the computational tools used in this work are described where special emphasis is laid on a generally understandable introduction of the local vibrational modes. In section 3, the shortcomings of the TEP are discussed whereas in section 4 the MLEP is introduced as a solution to the problem and its usefulness demonstrated for different groups of ligands. The chemical relevance of the new approach presented in this work is evaluated in section 5. The conclusions that can be drawn from this study are summarized in the last section.

## 2. COMPUTATIONAL METHODS SECTION

Since Tolman's approach has to be improved in a rigorous way, we will make three major changes with regard to his work: (i) Vibrational frequencies depend on the masses of the atoms participating in a vibrational movement. Therefore, we will base the analysis on force constants rather than the corresponding frequencies. Force constants exclusively depend on electronic factors and are suitable for providing a direct insight into bonding. (ii) All CO stretching modes of any metal carbonyl complex are contaminated by mode−mode coupling contributions. Therefore, we will replace the TEP values based on normal vibrational modes by their local, coupling-free counterparts, i.e., the LTEPs of Cremer and co-workers.[56] We will indicate the use of local stretching frequencies by LTEP$\omega$ and that of local stretching force constants by LTEPk in all those cases where there is a need to avoid confusion. (iii) It is desirable to replace an indirect descriptor by a direct descriptor of the intrinsic ML bond strength. To carry out this 3-step task, a basic understanding of the local vibrational mode is mandatory. Since the determination of the latter has been given in detail in the original literature,[84−87] we provide here a more general description of local, completely decoupled vibrational modes.

Vibrational modes are determined by a potential energy and a kinetic energy contribution, and as such mode−mode coupling


DOI: 10.1021/acs.inorgchem.5b02711
*Inorg. Chem.* 2016, 55, 2332−2344

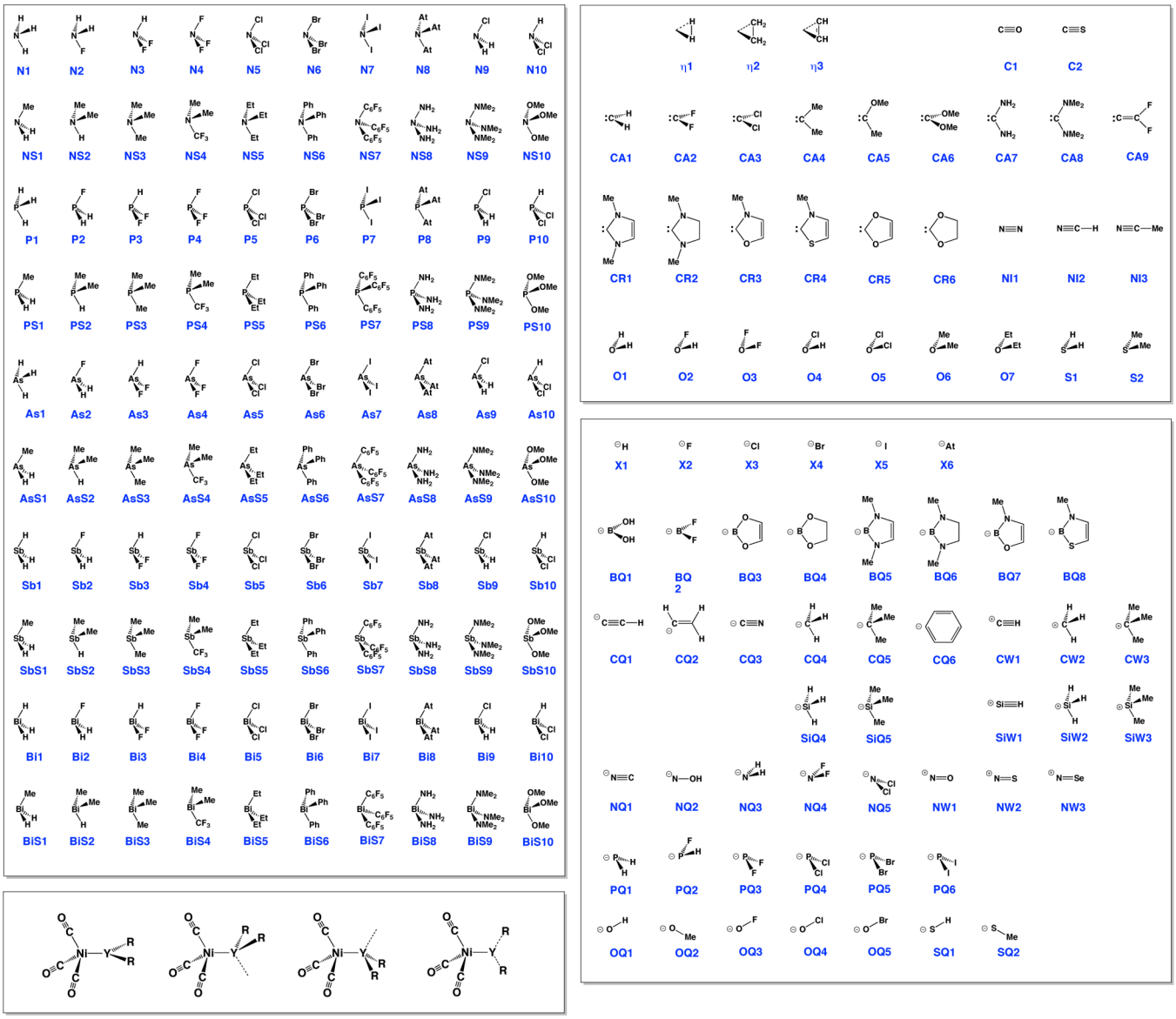


**Figure 1.** 181 nickel−carbonyl complexes L−$NiCO_3$ studied in this work. Each ligand is given a group name (e.g., N for amines, P for phosphines, As for arsines, etc.) and a number. The conformation of a complex is given by comparing the drawing of ligand L = $YR_2$ with the 4 conformational possibilities of the complex given in the lower left corner.

depends both on an electronic and a kinematic-coupling part as reflected by the off-diagonal terms of the force constant matrix (potential energy part) and those of Wilson's G-matrix (kinetic energy part), respectively.[88] Solving the Wilson equation of vibrational spectroscopy involves a diagonalization of the force constant matrix and thus eliminates electronic coupling. However, the normal vibrational modes obtained in this way are still kinematically coupled.[84] The problem of mode−mode coupling of the measured CO stretching vibrations was realized also by other authors[48] but could not be solved because the kinematic-coupling requires a reformulation of the Wilson equation.[84] Elimination of the latter coupling requires us to reformulate the Wilson equation by starting from the Euler−Lagrange equations in mass-decoupled form.[84] This leads to the Zou−Cremer local form of the Wilson equation, which can be solved to obtain electronically and kinematically decoupled local vibrational modes.[85,87] As shown by Zou and co-workers, there is a 1:1 relationship between normal and local vibrational modes,[85] and for each of the local modes a force constant $k^a$, a frequency $\omega^a$, a reduced mass, and an intensity[87] can be determined. Although not used in the current work, it is noteworthy that local mode frequencies can be obtained once normal-mode frequencies have been measured.[89−91] Equations leading to the local mode properties for molecules in their equilibrium geometry as well as for reacting molecules have been discussed in the original literature.[92]

Since the previous work on LTEPs[56] was carried out with the M06 functional, which was originally developed for the use in transition metal chemistry,[93] we also employed this XC functional in the current work. However, additional calculations were performed with the hybrid functionals B3LYP[94] and $\omega$B97X-D[95,96] which led to similar results although for some of the sterically congested Ni-complexes saddle points rather than minima were obtained. All calculations were carried out with Dunning's aug-cc-pVTZ basis sets.[97−99] For elements Sb, I, Bi, and At, the Stuttgart's effective core potentials (ECPs) were used in connection with the corresponding Dunning basis sets.[100,101] The DFT calculations were carried out using an ultrafine integration grid, which corresponds to 99 radial-shells and 590 angular-points per shell for each atom.[102]

Optimized geometries were obtained by applying tight criteria ($10^{-7}$ atomic units for forces and displacements) as well as tight convergence criteria for the self-consistent field calculations ($10^{-9}$ for the density matrix elements). In some cases (documented in the Supporting Information), the lowest vibrational frequencies became small, and


DOI: 10.1021/acs.inorgchem.5b02711
Inorg. Chem. 2016, 55, 2332−2344

long NiY bonds resulted, which indicated a van der Waals complex. For the purpose of keeping complete sets of amines, phosphines, etc., van der Waals complexes were kept in the comparison of the 181 complexes. For each complex investigated, the normal vibrational frequencies were calculated in the harmonic approximation. The normal modes were used to calculate the local stretching modes, the corresponding local force constants $k^a$s, local frequencies $\omega^a$s, and coupling frequencies $\omega_{coup}$s.[56] In the case of hapto-ligands, a dummy atom D at the center of the bond in question was used to obtain the local stretching mode between Ni and D. For an appropriate comparison of CEP, LTEP, and measured TEP values, the former two quantities were scaled using the calculated and measured 21 normal-mode frequencies of $Ni(CO)_4$ to derive suitable scaling factors.[56]

There are ligands that lower the overall symmetry of the Ni-complex from $C_{3v}$ to $C_s$ or even $C_1$ so that the choice of a suitable CO stretching mode is no longer unique. In these cases, the average local CO stretching frequency and average CO stretching force constant were taken as is mostly done in the literature (see Supporting Information).

The force constant $k^a$(AB) measures the intrinsic strength of the bond AB.[103−106] When comparing a large set of $k^a$ values, with the use of a relative bond strength order (BSO) $n$ is convenient.[103−106] The relative BSO $n$(ML) is obtained by utilizing the extended Badger rule,[106−108] according to which $n$ is related to the local stretching force constant $k^a$ by a power relationship, which is fully determined by two reference values and the requirement that for a zero-force constant $n$ becomes zero. In this work, we used as reference bonds the CuC bond in $CuCH_3$ as a bond close to a single bond and the NiC bond in $NiCH_2$ as a bond close to a double bond. To quantify the single or double bond character, the Wiberg bond orders[109,110] for these molecules were calculated to be $n$(Wiberg,CuC) = 0.848 and $n$(Wiberg,NiC) = 1.618, which corresponds to a ratio of 1.00:1.908. Utilizing the Wiberg bond orders, the following BSO relationship was derived

$$n = 0.480(k^a)^{0.984} \quad (1)$$

which was used for all NiY bonds as local force constants can be directly compared for different bonding situations involving elements throughout the periodic table.

It is important to note that the Wiberg index for the reference molecules is used here only to obtain a reasonable bond order value for the calibration of eq 1. The relative magnitude of the BSO values calculated would not change if $n$(Wiberg,NiC) = 2.00 would be taken. In general, there is no relationship between Wiberg bond indices (describing bond multiplicities) and relative BSO values (describing the intrinsic bond strength), which was verified in this work. Wiberg bond indices have no experimental counterpart whereas the BSO values, in principle, can be derived from measured frequencies and thereby have an experimental counterpart.

For smaller ligands, anharmonic corrections to the frequencies were also calculated utilizing second order vibrational perturbation theory (VPT2).[111] There were significant differences in the local mode force constants and frequencies; however, the BSO values obtained utilizing anharmonically corrected frequencies did not differ much from what is in line with our previous experience.[105,112] This is a result of the fact that reference and target molecules are affected by the anharmonicity corrections for the ML stretching frequency by comparable amounts. Therefore, a treatment of anharmonicity corrections, which would have been difficult or even impossible for many of the Ni-complexes investigated, was not further pursued.

The Ni−L and Ni−CO bonding mechanisms were investigated with the help of second order perturbation theory to determine hyperconjugative and anomeric delocalization energies.[113,114] For this purpose, the natural bond order (NBO) program NBO6[115] was employed. The latter was also used to determine atomic charges and Wiberg bond indices. Trends in bonding were described utilizing different electronegativity scales where Allred−Rochow electronegativities $\chi$ were favored because they include elements of the fifth and sixth period.[116,117]

The local mode analysis was carried out with the program package COLOGNE2015.[118] Although the major part of this work is based on the use of local stretching force constants, for each molecule all $3N - 6$ local modes were determined. The ACS (adiabatic connection scheme) program of Zou and Cremer[119] was applied to determine mode coupling frequencies $\omega_{coup}$. All DFT calculations were carried out using the Gaussian09[120] program package.

## 3. SHORTCOMINGS OF TOLMAN'S CONCEPT

All ligands investigated in this work are shown in Figure 1. A given ligand L can adopt different conformations where the most stable conformation is given at the bottom of Figure 1 (left side). Large $YR_3$ ligands prefer a staggered conformation relative to the $Ni(CO)_3$ group. However, in many cases such as L = $NF_3$, $PCl_3$, $As(C_6F_5)_3$, $SbI_3$, or $Bi(NH_2)_3$, an eclipsed conformation is preferred because of electrostatic attraction with the positively charged C atoms of the three carbonyl groups. Although the rationalization of the preferred equilibrium conformation in each case may be in itself an interesting topic, it is only of secondary importance in this work and will not be discussed. In Table S1 of the Supporting Information, the CO distance $R$, the local CO stretching frequency $\omega^a$, and local CO stretching force constant $k^a$ are listed for the 181 L−$Ni(CO)_3$ complexes investigated. For each L a descriptive acronym is given, which is used for a rapid identification of a complex in several of the figures presented in this work. Also given are the symmetry of the Ni-complex, the atom Y directly bonded to Ni, and the four calculated parameters characterizing the NiY bond: $R$(NiY), $k^a$(NiY), $\omega^a$(NiY), and BSO value $n$(NiY). In the following, we will refer to Ni−L or metal−ligand bonding if metal−ligand interactions are considered in a general way whereas detailed information is provided when considering the Ni−Y bond with Y being that atom of the L being directly bonded to Ni.

## 4. INFLUENCE OF MODE−MODE COUPLING

Crabtree and co-workers[48] tried to justify the TEP by calculating CEP values for a set of 65 L−$Ni(CO)_3$ complexes. They realized that mode−mode coupling might lead to errors in the TEP but failed to remove the kinematic-coupling between the CO stretching vibrations and other vibrations.[56] As indicated by Kalescky and co-workers,[56] the TEP is significantly flawed by mode−mode coupling. Here, we quantify this result by showing the correlation of TEP and CEP values[48] with the correct LTEP where the calculated values are scaled to adjust the harmonic approximation of the normal-mode frequencies to the measured CO stretching frequencies.

In Figure 2, the TEP and CEP for the Crabtree test set of 66 ligands is scrutinized utilizing the LTEP as a reliable parameter. If there would be no mode−mode coupling in the case of the CO stretching mode as was originally assumed by Tolman, all TEP (or CEP) values would lie on the dashed line. This turns out to be an incorrect assumption as the TEP (red dots in Figure 2) and the CEP (blue dots) values are on two lines shifted and inclined (ascend of the correlation line 0.77 and 0.82 $cm^{-1}$, respectively) with regard to the dashed green line representing the coupling-free situation ($R^2$ = 0.985 and 0.981; $\sigma$ = 5.7 and 6.8 $cm^{-1}$, respectively). The deviation of the TEP and CEP values from the corresponding LTEP$\omega$ values is a result of mode−mode coupling, which leads to different CO coupling frequencies (see Figure 3). Qualitatively an inverse relationship between coupling frequencies and the local CO stretching frequencies is fulfilled, i.e. the smaller CO stretching



DOI: 10.1021/acs.inorgchem.5b02711
Inorg. Chem. 2016, 55, 2332−2344

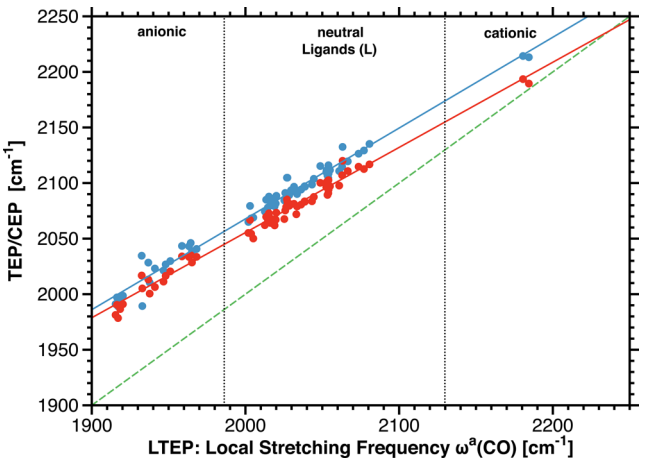


**Figure 2.** Comparison of measured TEP and in this work calculated CEP values with the corresponding LTEP$\omega$ values for the Crabtree test set of 66 L–Ni(CO)$_3$ complexes ($R^2$ = 0.985 and 0.981; $\sigma$ = 5.7 and 6.8 cm$^{-1}$, respectively). The dashed green line gives the ideal correlation for coupling-free TEP and CEP values. Complexes with anionic ligands L are found in the low range, with neutral L in the middle, and with cationic L in the high frequency range as indicated in the figure.

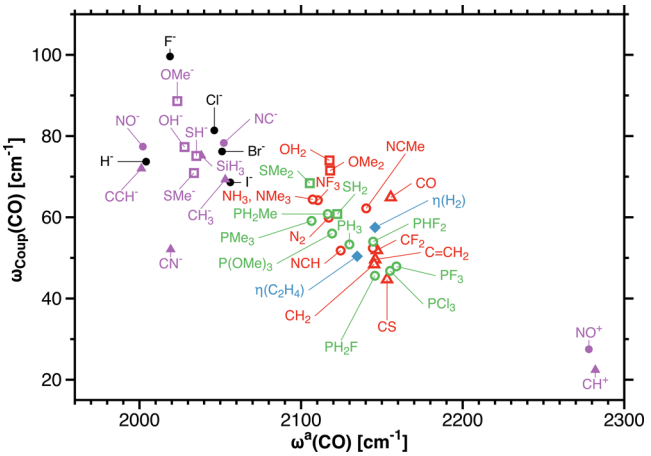


**Figure 3.** Coupling frequencies $\omega_{coup}$ of the CO stretching mode given for a set of selected ligands L of complexes L–Ni(CO)$_3$ are compared with the corresponding (uncoupled) local CO stretching frequencies $\omega^a$. The TEP is more strongly contaminated by the $\omega_{coup}$ frequencies for weaker Ni–L bonds.

frequency $\omega^a$(CO) implies a larger mode–mode coupling where $\omega_{coup}$(CO) can increase from 20 (cations) to 100 (anions) cm$^{-1}$. This reveals that the TEP and any parameter derived from it (either measured or calculated) is flawed by mode–mode coupling.

Mode–mode coupling cannot be predicted without using local vibrational modes because it depends on the nature of the M–L bond, which seems to vary even for the same type of ligand. Clearly, the sensitivity of the TEP or CEP is smaller than that of the mode decoupled LTEP$\omega$ as coupling frequencies contaminate the lower CO stretching values more than the higher ones. Clearly, the TEP is just a qualitative indirect measure of the M–L bond strength where detailed knowledge of its deficiencies might help experimentalists to apply it in a useful way. However, in the next subsection we will show that the TEP is even severely flawed as a qualitative M–L bond strength parameter so that it becomes useless.

**Is There a Relationship between C≡O and M—L Bonding?** We have investigated this question for the 181 L–NiCO$_3$ complexes shown in Figure 1 by calculating the local Ni–L and CO stretching force constants and comparing them in Figure 4. The $k^a$(CO) and $k^a$(NiY) values scatter so strongly

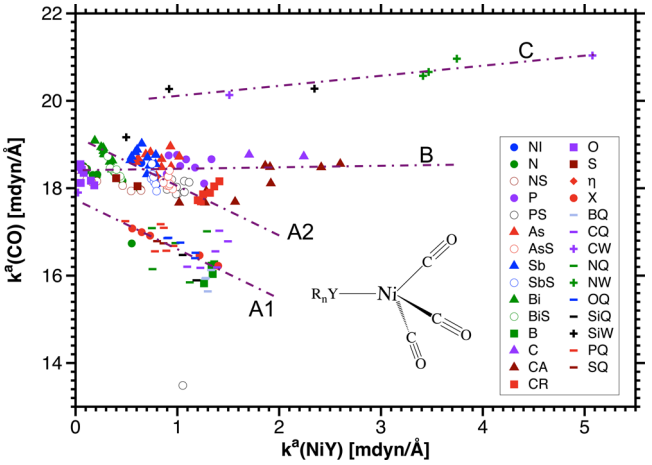


**Figure 4.** Testing of the relationship between NiL and CO bond strength for 181 nickel–carbonyl complexes L–NiCO$_3$ utilizing the corresponding local stretching force constants, i.e., comparing $k^a$(CO) and $k^a$(NiY) values. Some possible relationships (A, B, C) are indicated by dashed lines. Each group of ligands is indicated by a colored symbol. Compare with Figure 1.

that a quantitative relationship can be excluded. With a focus on subgroups of ligands (as indicated by special colored symbols, compare with Figure 1) the qualitative trends A, B, and C can be distinguished. There are several A-type relationships (inverse relationships between $k^a$(CO) and $k^a$(NiY)), i.e. with increasing strength of the M–L bond the CO bond becomes weaker. This can be interpreted in the sense of Tolman who pointed out that an increase of electron density at the Ni atom leads to strong $\pi$-back-donation, thereby an increased population of the CO antibonding $\pi$-orbital, and a weakening of the CO bond reflected by a decrease of the CO stretching frequency. Any increase of the ML bond strength implies either stronger $\sigma$-donation of L to M or an increase in the ML bond strength due to $\pi$-donation from L to M, which are both in line with Tolman's idea.

Although two type A relationships (A1 and A2) seem to hold when all data points are considered, closer inspection reveals that the halogenides (X: red balls) are the only group of ligands that follows a type A behavior. All other ligands investigated quantitatively and qualitatively deviate from a type A relationship; i.e., the TEP is only useful for the 5 halogenides, and for the other 176 ligands investigated it does not hold.

Relationships of type B indicate that there is no change in the CO bond strength when the Ni–L bond becomes stronger. Some carbene and phosphine ligands follow this trend as do the ligands CO and CS. However, there is not a single group of ligands that can be identified as type B ligands, and therefore, it is otiose to search for electronic reasons causing type B behavior. There are several relationships of type C (only one is shown in Figure 4), which predict for an increase of the ML bond strength an increase of the CO bond strength (contrary to what Tolman predicted). This is found for cationic ligands, but also for Arduengo carbenes (red squares) and other carbenes. This implies that back-donation from Ni to the L


DOI: 10.1021/acs.inorgchem.5b02711
Inorg. Chem. 2016, 55, 2332–2344

lowers the density at Ni and thereby reduces $\pi$-back-donation to CO. The reasons for this kind of NiL back-donation are discussed in the following.

No matter whether type A, B, or C relationships are assumed there is always a (strong) scattering of data points apart from a few exceptions such as the halogenides or the Arduengo carbenes. We conclude that Figure 4 provides proof that Tolman's idea of an inverse relationship between NiL and CO bonding is not correct in general and even for the phosphine ligands (purple dots in Figure 4) it is fulfilled. Among the 181 different ligands investigated, it is only for the five halogenides (L = F, Cl, Br, I, At) that the expected inverse relationship between TEP and the intrinsic ML bond strength can be derived, whereas for the 6 Arduengo carbenes a direct relationship results contrary to Tolman's expectations. In such a situation, it seems to be more appropriate to replace TEP, CEP, or LTEP$\omega$ by an electronic parameter that provides a direct measure of the ML bond strength.

## 5. METAL–LIGAND ELECTRONIC PARAMETER: MLEP

The $A_1$-symmetrical CO stretching frequency was chosen by Tolman because it can be easily measured in most cases. Nowadays, a more direct vibrational characterization of ML bonding is facilitated by the availability of terahertz spectroscopy or depolarized Raman scattering, and in this regard the current investigation is timely. With the recent advances in terahertz spectroscopy,[121−123] far-infrared absorptions down to 40 $cm^{-1}$ can be recorded, and with this, the measurement of the ML stretching frequencies becomes feasible. Many metal−ligand stretching frequencies are in this region, and of course, they are often coupled. However, one can apply terahertz spectroscopy in connection with the local mode analysis of Konkoli and Cremer, determine the local ML stretching force constants $k^a$ utilizing measured frequencies,[89−91] and use the $k^a$(ML) values rather than the TEP as a reliable M−L describing electronic parameter, henceforth called MLEP. Alternatively, and carried out in this work, one can calculate the MLEP using a reliable quantum chemical method. Once the local ML stretching force constant $k^a$(ML) is known, one can simplify comparison by deriving BSO values (see the Computational Methods Section).

In Figure 5, the relative BSO values of all NiY bonds (of NiL) are given as a power relationship of the calculated local stretching force constants $k^a$(NiY). BSO values between 0.75 and 1.25 are considered as normal; those with 0.25 < BSO < 0.75 are weak, and those with 0 < BSO < 0.25 are very weak. Strong NiY bonds have a BSO > 1.25, and very strong NiY bonds have BSO > 2.0 where this characterization has the purpose to facilitate the discussion on the basis of the MLEP defined via the local stretching force constants $k^a$(NiY) and the corresponding BSO values. In the following, we will analyze the MLEP for groups of closely related ligands separately to determine those electronic factors, which either increase or decrease the intrinsic nickel−ligand bond strength.

**Intrinsic Strength of Nickel−Phosphine Bonding.** In Figure 6, the BSO values of 20 phosphines are compared (see also Supporting Information), which vary by 0.26 BSO units in the range 0.38 < BSO < 0.64. Phosphine, $PH_3$, leads to a relatively low BSO(Ni−P) value of 0.431 as the H is more electronegative than P thus reducing its $\sigma$-donor capacity of the phosphine. Accordingly, one expects that the $\sigma$-donor capacity of $PF_3$ is even weaker than that of $PH_3$ because of the increased electronegativity of F compared to H. In contrast, the BSO

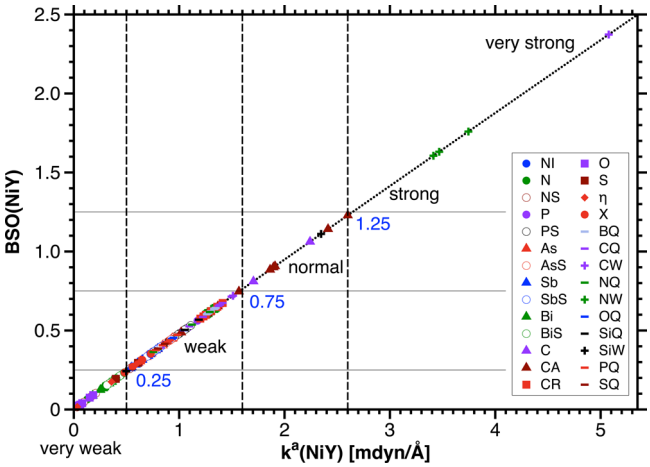


**Figure 5.** Relative NiY bond strength orders (BSOs) are given for 181 L−Ni(CO)$_3$ complexes as a function of the local stretching force constant $k^a$(NiY). Regions of normal, strong, very strong, weak, and very weak Ni−Y bond strengths are indicated by dashed horizontal lines where the NiC bond strength of Ni(CO)$_4$ is used as a suitable reference (relative BSO: 0.811).

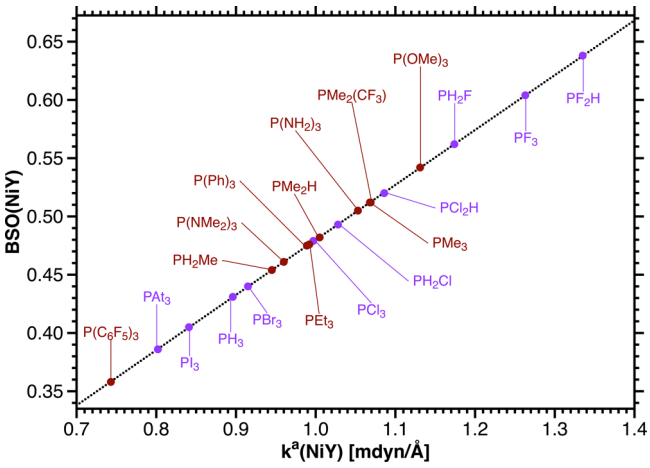


**Figure 6.** Relative Ni−P BSOs of phosphine-nickel tricarbonyl complexes, $R_3PNi(CO)_3$, are given as a function of the local stretching force constant $k^a$(Ni−P) . Halogenated phosphines are given by the purple color and all others by the brown color.

value increases to 0.604 which is higher than that of all other trihalogenophosphines (Figure 6, Table S1). Clearly, synergetic bonding rather than just $\sigma$-donor bonding plays a decisive role and leads to a strong increase in the BSO value. As shown in Figure 7, a 3d(Ni) electron pair can delocalize into a low-lying pseudo-$\pi$*(PF) orbital thus increasing the Ni−Y bond strength. The degree of $\pi$-back-donation from metal to ligand depends on (i) the energy of the pseudo-$\pi$*(PX) orbital (X = F, Cl, Br, I, At), which is lower and closer to the 3d(Ni)-orbitals as the electronegativity of the halogen X is higher, and (ii) the overlap between the 3d(Ni)-orbital involved and the 3p$\pi$(P)-orbital contributing to the pseudo-$\pi$*(PX)-orbital. The 3p$\pi$(P)-coefficient of the pseudo-$\pi$*(PX) orbital is large if the PX polarity is large (as a result of the orthogonality between pseudo-$\pi$($PX_m$) and pseudo-$\pi$*($PX_m$) orbital), i.e., the larger electronegativity of X implies a larger overlap, stronger back-donation to the ligand and thereby a larger Ni−L bond strength. Hence, back-donation to L should decrease in the series F, Cl, Br, H ∼ I, At.



DOI: 10.1021/acs.inorgchem.5b02711
Inorg. Chem. 2016, 55, 2332−2344

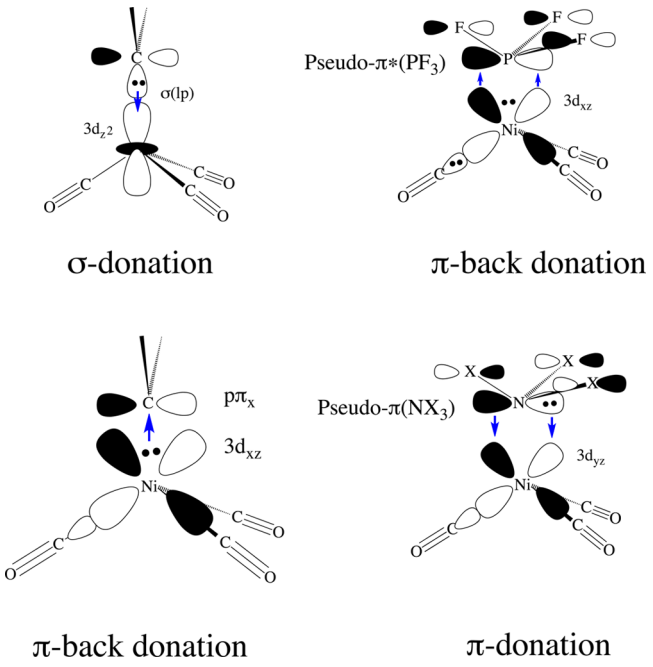


**Figure 7.** Interactions between ligand L and the $Ni(CO)_3$ group: $\sigma$-donation from the lone-pair orbital of a carbene to the $3d_{z^2}$(Ni)-orbital (upper left); $\pi$-back-donation to the pseudo-$\pi^*$ orbital of $PF_3$ (upper right); $\pi$-back-donation to the $2p\pi$-orbital of a carbene (lower left); $\pi$-donation from an occupied pseudo-$\pi$ orbital of $NX_3$ to an empty 3d(Ni)-orbital (lower right).

The calculated trend in BSO values, $PAt_3$ < $PI_3$ < $PH_3$ < $PBr_3$ < $PCl_3$ < $PF_3$ (Figure 6), suggests that $\pi$-back-donation to the trihalogenophosphine is decisive and that $\sigma$-donation is more a second order, but nevertheless important, effect [$\sigma$-bonding would increase from F($\chi$ = 4.10) to Cl(2.83), Br(2.74), H(2.20) ~ I(2.21), and At(1.90[116,117])]. If $\sigma$-donation would be more important, then the BSO values of $PH_3$ and $PI_3$ would be similar (considering that back-donation becomes weak for these phosphines). Their difference suggests that other effects such as steric bulk (strongly increasing from $PH_3$ to $PI_3$ and $PAt_3$ and thereby weakening the Ni−Y bond) or relativistic effects [contraction of the 5s(I),5p(I) and 6s(At),6p(At) orbitals implies a smaller $3p\pi$(P) coefficient in the pseudo-$\pi^*(PX_3)$ orbital and reduced back-donation from Ni to L] also play a role.

The unexpected NiP BSO value of 0.638 for $PF_2H$ marks the strongest Ni−P bond in the series of phosphines investigated. It is due to the optimal compromise between moderate weakening of $\sigma$-donation (small number of electronegative substituents X) and strong $\pi$-back-donation (two electronegative F atoms). Ligand $PH_2F$ is optimal with regard to $\sigma$-donation, but less effective with regard to $\pi$-back-donation and therefore has a BSO of 0.562, which is lower than that of $PF_3$ (0.604; Table S1). A somewhat different trend is found for the chlorinated phosphines, $PCl_3$ < $PClH_2$ < $PCl_2H$ (<$PH_2F$), which indicates that the reduced electronegativity of Cl leads to less effective $\pi$-back-donation and weaker Ni−P bonds.

$\pi$-Back-donation plays also a role for the trimethoxy ($n$ = 0.542), triamino (0.505), and tridimethylamino substituted phosphines (0.461, Figure 6) and places them between the fluoro and iodo substituted phosphines. In the case of alkyl or aryl substituted phosphines, $\sigma$-donation and steric repulsion have to be considered to understand the intrinsic NiY bond strength in the corresponding complexes. For example, in the series $PH_2Me$ (0.454) < $PHMe_2$ (0.482) < $PMe_3$ (0.512) ~ $PMe_2CF_3$ $\sigma$-donation seems to increase because of the donor effect of the methyl group whereas steric effects are less important for NiY bonding in these cases. A phosphine with a $CF_3$ substituent should be a weaker $\sigma$-donor. This is not reflected by the BSO values of $PMe_3$ and $PMe_2CF_3$. Hence, the $\pi$-back-donation effect cannot be excluded even for the alkyl substituted phosphines as it would increase for the $CF_3$ group: The C atom ($\chi$ = 2.50 compared to $\chi$(P) = 2.06) becomes more electronegative thus supporting $\pi$-back-donation and offsetting a reduction of $\sigma$-donation, which leads to the similarity of the BSO values of methyl and $CF_3$ substituted phosphines.

Steric repulsion between L and the carbonyl ligands is the cause for the relatively low BSO values of $PEt_3$ (0.476) and $PPh_3$ (0.475). Even lower values of 0.461 for $P(NMe_2)_3$ and 0.358 for $P(C_6F_5)_3$ are due to steric weakening of the Ni—P bond strength despite potential stabilization by $\pi$-back-donation in the first case (see above) or F,C(≡O) attraction in the second case. This underlines an important advantage of the MLEP when compared with the TEP. Tolman[2] saw the necessity of complementing the CO stretching frequency by a geometric measure, which provides, in the form of a cone angle, a measure for the steric effect of a ligand. A steric parameter, which is just qualitative in nature as a quantitative relationship between cone angle and the strength of the metal−ligand bond, is difficult to find, and becomes superfluous as the MLEP based on the local NiY stretching force constant includes all electronic and steric factors influencing the ML bond strength.

**Intrinsic Strength of Nickel−Amine Bonding.** In Figure 8, the BSO values of 20 amine ligands are compared, which vary in the range 0.02 < BSO < 0.32 by 0.30 BSO units. On the average, amines are 0.3−0.4 BSO units less strongly bonded to Ni than the corresponding phosphines, which clearly has to do with the larger electronegativity of N ($\chi$ 3.07 compared to P 2.06) thus making it a weaker $\sigma$-donor and a poorer $\pi$-acceptor. For comparison, the BSO values of two nitrile ligands are also

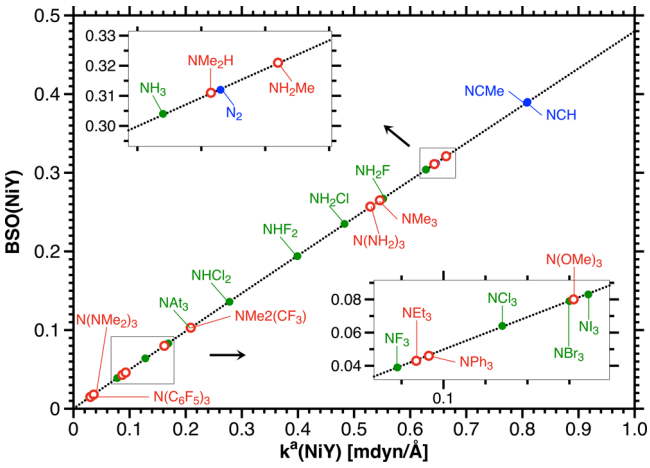


**Figure 8.** Relative Ni−N BSOs of amine-nickel tricarbonyls, $R_3N$−$Ni(CO)_3$, are given as a function of the local stretching force constant $k^a$(Ni−N). Halogenated amines are indicated by the green color, all others by the red color. The clustering of data points in the region 0.03 < BSO < 0.09 and 0.295 < BSO < 0.325 is enlarged in the insets. For reasons of comparison, the BSO values of two nitrile ligands and $N_2$ acting as a $\sigma$-donor are also given (blue color).



DOI: 10.1021/acs.inorgchem.5b02711
Inorg. Chem. 2016, 55, 2332−2344

shown, which are stronger $\sigma$-donors as reflected by BSO values close to 0.39.

There are four electronic effects, which play an active role according the NBO analysis (see also Figure 7). (i) $\sigma$-Donor ability: The $\sigma$ donor ability of an amine $NX_3$ decreases with increasing electronegativity of X. (ii) Size of X: Because of the relatively small Ni,N distance of about 2.2 Å (see $NMe_2H$ in Table S1), the size of the halogen X matters. Steric interactions increase in the series F, Cl, Br, I, At. (iii) $\pi$-Acceptor ability: The $NX_3$ $\pi$-acceptor ability is lower than that for $PX_3$ and decreases significantly if $\chi(X) < \chi(N)$ [the orbital overlap is reduced and the pseudo-$\pi^*(NX_3)$ orbital is higher in energy; see below]. (iv) $\pi$-Donor ability: $NX_3$ can act as a $\pi$-donor by delocalizing pseudo-$\pi(NX_3)$ electrons into an empty Ni orbital (see Figure 7).

The decrease in the $\pi$-acceptor ability can be understood if one realizes that most amine substituents, apart from the fluoro substituted ones, have a lower electronegativity than N, which implies that the $2p\pi(N)$ coefficient in the pseudo-$\pi^*(NX_3)$ orbital is of small magnitude and reduced overlap between the latter and the corresponding 3d(Ni) orbital results. The reverse holds for the $2p\pi(N)$ coefficient in the pseudo-$\pi(NX_3)$ orbital. Amines $NX_3$ with I or At have stronger NiN bonds because of stronger $\sigma$- and $\pi$-donor ability where steric repulsion can also influence the order of intrinsic Ni,N bond strengths: $NF_3$ < $NBr_3$ < $(NCl_3)$ < $NI_3$ < $NAt_3$.

Steric effects are also responsible for the low BSO values of $N(NMe_2)_3$ or $NEt_3$ (0.018 and 0.043). If the donor ability is increased by methyl groups, BSO values as large as 0.32 result. It is noteworthy that fluoroamine leads to a stronger NiN bond (0.267) than chloroamine (0.235), which reveals that 3d(Ni) $\pi$-back-donation into a sufficiently low-lying pseudo-$\pi^*$(NHF) orbital still outweighs other effects such as the disadvantage in $\sigma$-donation involving the lone-pair electrons lp(N) (Table S1). $NH_3$ and its methyl substituted derivatives turn out to be the strongest $\sigma$-donors with the strongest Ni–N bond (BSO values of 0.304–0.321) lowered only somewhat for trimethylamine because of steric hindrance (slightly elongated R(NiN) distance of 2.204 Å). For $NEt_3$, R(NiN) increases to 2.966 Å and gets close or beyond a typical van der Waals distance of 3.77 Å in the case of $NPh_3$ (R = 3.591) or $N(C_6F_5)_3$ (4.385 Å, where $Ni(CO)_3$ and L attract each other just weakly [$NEt_3$, BSO = 0.043; $NPh_3$, BSO = 0.046; $N(C_6F_5)_3$, BSO = 0.015 with local NiN stretching frequencies of just 115, 119, and 67 $cm^{-1}$, respectively, and very small local stretching force constants; Table S1].

**Intrinsic Strength of Nickel-Arsine, -Stibine, and -Bismuthine Bonding.** Since for the five pnicogen-containing L groups the same 20 $YX_mH_{3-m}$ or $YR_mH_{3-m}$ ligands have always been used in this work, they can be directly compared with regard to the range of BSO values, their average, the range width, and the R(NiY) distance given in Å for $YH_3$ (the latter three values in parentheses), which are given in the following: 0.015–0.321(N: 0.148; 0.306; 2.165); 0.386–0.638 (P: 0.487; 0.252; 2.264); 0.297–0.489 (As: 0.409; 0.192; 2.391); 0.261–0.399 (Sb: 0.346; 0.138; 2.566); and 0.088–0.233 (Bi: 0.168; 0.145; 2.745) (see Figures 9–11).

The increasing electropositive character of the pnicogen atoms with increasing atomic number [$\chi$ values for N, P, As, Sb, Bi: 3.07, 2.06, 2.20, 1.82, 1.67; the relatively large $\chi$(As) is due to the d-block contraction, which leads to an ineffective shielding of the nucleus and an enlargement of $\chi$(As)] should make them better $\sigma$-donors. But the 3d–np$\sigma$-overlap is

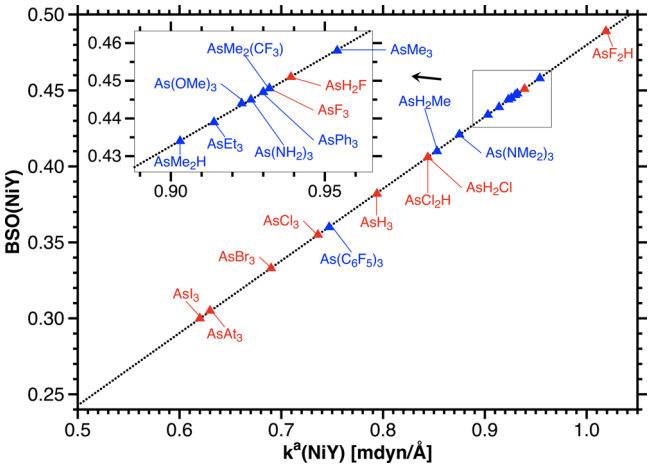


**Figure 9.** Relative Ni–As BSOs of arsine-nickel tricarbonyls, $R_3As$–$Ni(CO)_3$, are given as a function of the local stretching force constant $k^a$(Ni–As). Halogenated arsines are given by the red color, all others by the blue color.

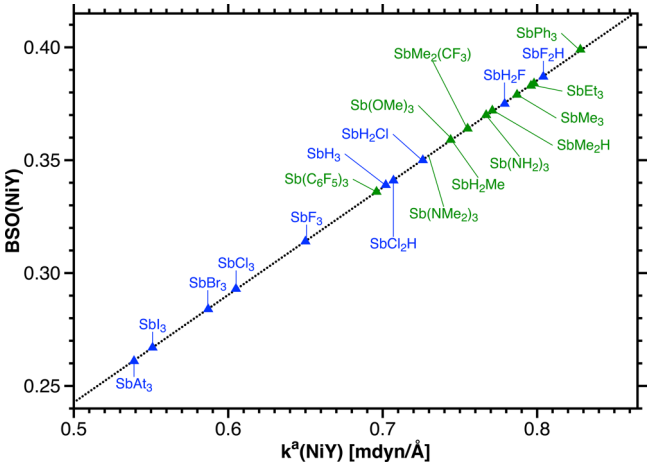


**Figure 10.** Relative Ni–Sb BSOs of stibine-nickel tricarbonyls, $R_3Sb$–$Ni(CO)_3$, are given as a function of the local stretching force constant $k^a$(Ni–Sb). Halogenated stibines are given by the blue color, all others by the green color.

increasingly reduced in the series 3d(Ni)–3p(P), –4p(As), –5p(Sb), –6p(Bi) due to larger R(NiY) values, and there is increasing mismatch of the orbitals involved. Also, $\pi$-back-donation to pseudo-$\pi^*(YX_m)$ orbitals, which is optimal for P, plays an increasingly smaller role for higher atomic numbers of Y so that BSO values spread over a smaller and smaller range (0.306 for N but just 0.145 for Bi) and the average BSO value drops from 0.487 in the case of P to 0.168 in the case Bi.

For the arsines and stibines (Figures 9 and 10), it is equally true that $\pi$-back-donation to a pseudo-$\pi^*(YX_mH_{3-m})$ ($m$ = 1,2, 3) orbital dominates bonding as in the case of the phosphines, which leads to a similar increase of the BSO values from X = At to F ($m$ = 3) and leads to better $\sigma$-donation if halogens are replaced by H atoms. Since the $\pi$-donor effect becomes less and less dominant, the variation in the BSO values decreases. Since the NiY distances increase from Y = P to Sb (see Table S1 and above), steric repulsion is reduced, and $YR_3$ ligands with bulky, but $\sigma$-donation increasing R move to larger BSO values.

For the bismuthines, Ni–Y bonding is predominantly based (as in the case of Y = N) on the $\sigma$-donor ability of the ligand where, however, this is significantly reduced because of the



DOI: 10.1021/acs.inorgchem.5b02711
Inorg. Chem. 2016, 55, 2332–2344

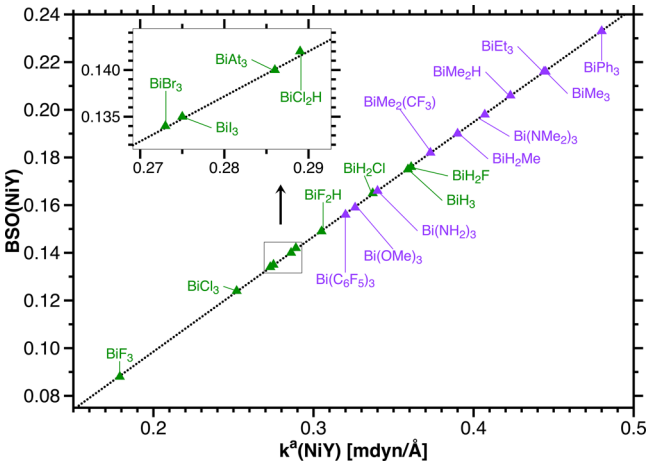


**Figure 11.** Relative Ni−Bi BSOs of bismuthine-nickel tricarbonyls, $R_3Bi-Ni(CO)_3$, are given as a function of the local stretching force constant $k^a$(Ni−Bi). Halogenated bismuthines are given by the green color, all others by the purple color. The clustering of data points in the region 0.132 < BSO < 0.138 is enlarged in an insert.

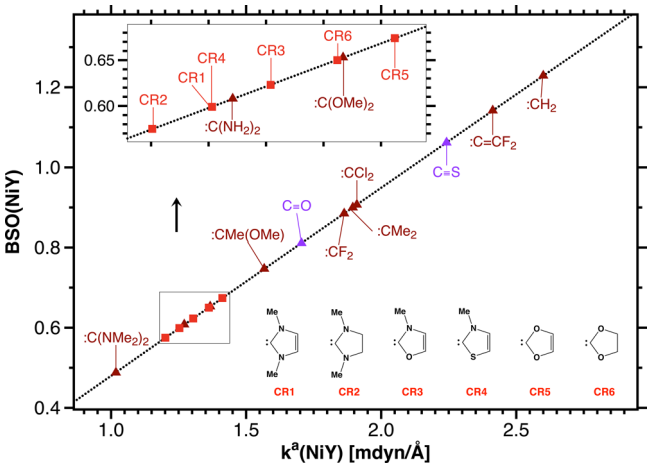


**Figure 12.** Relative Ni−C BSOs of carbene-nickel tricarbonyls, $R_2C-Ni(CO)_3$, are given as a function of the local stretching force constant $k^a$(Ni−C). CO and CS are also included (purple color), and normal carbenes (brown color) are distinguished from Arduengo carbenes (red color). The clustering of data points in the region 0.57 < BSO < 0.68 is enlarged in the inset.

scalar relativistic contraction of the 6s,6p orbitals of Bi. The latter is responsible for the low BSO(Bi−Y) values, which vary by just 0.145 from 0.088 to 0.233 so that they do not overlap with the stibine or arsine BSO values. Any electronegative bismuthine substituent reduces this low donor ability further, which leads to the following BSO values: $BiF_3$ < $BiCl_3$ < $BiBr_3$ < $BiI_3$ < $BiAt_3$ < $BiH_3$.

$\pi$-Back-donation to pseudo-$\pi^*(BiX_m)$ orbitals does play only a minor role because the electropositive Bi leads to a relatively high orbital energy. It becomes decisive only for $BiH_2F$ or $BiH_2Cl$, which have relatively high BSO values. With the increasingly larger $R$(Ni−Y) values (Y = As, Sb, Bi), steric repulsion is reduced for the bismuthine complexes so that ligands such as $BiEt_3$, $BiMe_3$, or $BiMe_2H$ can fully bring into play their increased $\sigma$-donor ability leading to BSO values of 0.216, 0.216, or 0.206.

**Intrinsic Strength of Nickel−Carbene Bonding.** Singlet carbenes have an lp for $\sigma$-donation and an empty p$\pi$-orbital for accepting negative charge from Ni. Therefore, the BSO value of L = $CH_2$ is with 1.229 the largest of all neutral ligands. Replacement of H atoms by hyperconjugative or $\pi$-donor substituents R = R′ leads to a reduction of the NiC bond strength, $R$: =$CH_2$ group (vinylidene; 1.142), Me (0.900), Cl (0.907), F (0.885), OMe (0.653), $NH_2$ (0.608), $NMe_2$ (0.488), etc. The Arduengo-type carbenes are interesting, and when they have the chance to form a delocalized 6$\pi$-system, withdraw negative charge from Ni thus increasing the strength of the Ni−C bond. For 5-membered rings with O atoms in $\alpha$-position the withdrawal is stronger (CR5:0.674) than for those with N atoms (CR1:0.599; Table S1 and Figure 12). The comparison of $k^a$(CO) and $k^a$(NiC) values in Figure 4 reveals that Arduengo carbenes represent a group of ligands that have a reverse rather than an inverse CO,NiY-relationship. This explains why in many cases the bonding of Arduengo carbenes to the metal is difficult to explain on the basis of the TEP values.[38,55,76,80,83,124−126]

Bulky groups lower the BSO value effectively because of the relatively small NiC bond length (1.9−2.0 Å). It is noteworthy that the CO and CS ligand lead to BSO values of 0.811 and 1.062. They are comparable in their NiC bond strength to that of substituted carbenes.

**Intrinsic Strength of Bonding between Nickel and Ionic Ligands.** The strongest NiY bonds are found for cationic ligands with empty p$\pi$-orbitals such as the methylidyne cation $CH^+$ (BSO = 2.373; strongest of all NiY bonds) that has a $\sigma$-lone pair and two empty p$\pi$-orbitals. The methyl cation leads to a BSO of just 0.720 whereas the t-butyl cation has a small BSO of 0.409. In the first case, the lowering of the BSO value is due to the missing $\sigma$-lp electrons whereas in the second case the steric bulk of the ligand hinders the acceptance of negative charge from Ni [increase of $R$(NiC) from 1.651 ($CH^+$), to 1.963 ($CH_3^+$) and 2.061 Å ($CMe_3^+$; Table S1)]. Inspection of the calculated geometry of the complex with the t-butyl cation ligand reveals that bonding is actually established by agostic interactions between CH bonds and the Ni atom. High BSO values are also found for $NO^+$ (1.759), $NS^+$ (1.631), and $NSe^+$ (1.606).

Compared to the values for the cationic ligands, variation of the BSO values of the anionic ligands is much smaller. Useful insight is provided by the analysis of the NiX bond strength for the halogenide anions $X^-$. Unexpectedly, the NiF bond strength is larger than that of all other halogenide anions (BSO = 0.583) despite a small $R$(NiF) of 1.991 Å, which should lead to destabilization because of lp,lp-repulsion between Ni and F. If this lp,lp-repulsion is absent as in the case of the hydride anion, the BSO value increases to 0.669 ($R$ = 1.579 Å). According to the NBO analysis, the high BSO(NiF) value is due to the delocalization of lp(F) electrons. In the case of halogenide ligands with higher atomic numbers, delocalization into an empty Ni valence orbital is reduced because of smaller overlap and an increase in the lp(X) orbital energy. For Cl, Br, and I, the BSO values drop to 0.353, 0.314, and 0.270 thus reflecting, despite an increase in $R$ (from 2.391 to 2.714 Å, Table S1), increased lp,lp repulsion and vanishing lp(X)−Ni delocalization possibilities.

Ligands of carbanionic character vary between 0.526 ($CMe_3^-$) and 0.714 ($HCC^-$) where steric interactions cause a decrease in the NiY bond strength. Amide and phosphide anions lead to less strongly bonded L−Ni(CO)$_3$ complexes (see Figure 13). It is noteworthy that $PF_2^-$ is the most strongly bonded phosphide anion ligand, which again underlines the


DOI: 10.1021/acs.inorgchem.5b02711
Inorg. Chem. 2016, 55, 2332−2344

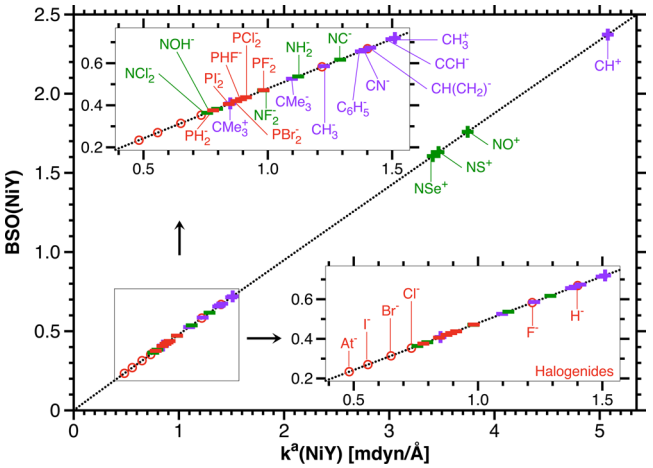


**Figure 13.** Relative NiC (purple), NiN (green), and NiP (red) BSO values of ionic ligands are given as a function of the local stretching force constant $k^a$(NiY). The clustering of data points in the region 0.25 < BSO < 0.75 is enlarged in two inserts where the inset in the lower right corner features the halogenide anions (red circles).

important role of $\pi$-back-donation from a 3d(Ni) orbital into the pseudo-$\pi^*(PF_2)$-orbital.

**Intrinsic Strength of Bonding between Nickel and Other Ligands.** Apart from the ligands explicitly discussed here, we have also investigated ligands leading to NiB, NiO, NiSi, or NiS bonding. Boron-containing ligands resemble in their bonding characteristics those of the carbocations ($\pi$-acceptors, however, no longer $\sigma$-donors; BSO values: 0.603−0.643; Table S1). Water and ethers are only weakly bonded (BSO values: 0.024−0.091; Table S1) whereas oxide anions have larger BSO values (0.447−0.502) because of their stronger $\sigma$-donor capacity.

The remarkable strength of Ni-hapto bonding (BSO: 0.175−0.306) is interesting, which is based on the donor capacity of a $\pi$-bond (ethene, acetylene) or $\sigma$-bond ($H_2$). It is noteworthy that the donor capacity of $H_2$ is larger (0.306) than that of ethene (0.287) or acetylene (0.175). Molecular nitrogen is a weaker donor via its $\pi$-bonds than via its lp-electrons (0.017 vs 0.312).

**Steric Effects: Is There a Need for a Second Electronic Parameter?** There are exchange repulsion and electrostatic interactions between the ligand L and the $Ni(CO)_3$ group. As far as these interactions influence the NiY bond strength, they are directly absorbed by the stretching force constant $k^a$(NiY) and reflected by the BSO value. In this respect, there is no need to determine a second electronic parameter as done by Tolman in form of the cone angle, which measures the steric bulk of a ligand L.

If there is a need to separate steric effects from other electronic effects, this can be easily achieved with the help of the local C−Ni-L bending force constant $k^a$(CNiL). The value of $k^a$(CNiL) will be large in the case of steric repulsion (indicating the rigidity of the ligand structure) whereas ligands L with little space requirements will be characterized by small $k^a(CNiL)$ values. In this way, an ordering of all L according to their steric bulk is easily possible. It would be beyond the scope of this work to develop a suitable bending order based on $k^a$(CNiL) values and to discuss for each ligand to which extent steric interactions influence the intrinsic NiY bond strength.

## 6. CONCLUSIONS

In a careful investigation of 181 nickel-tricarbonyl complexes L−Ni$(CO)_3$, we have determined for each L = $YR_m$ ($m$ = 0, ..., 3) the local CO and NiY stretching frequencies and force constants. As the former depends always on the masses of the atoms involved in a molecular vibration, we have focused on the more reliable stretching force constants, which directly relate to the electronic features of the vibrating bond and thereby its intrinsic bond strength. The quantum chemical investigation of the Ni-complexes and their vibrational properties has led to the following results. (1) Despite many simplification schemes, the vibrational modes of a transition metal complex always couple so that normal-mode frequencies are always contaminated by coupling frequencies. This problem can be solved by converting the normal vibrational modes into local vibrational modes as has been described by Konkoli and Cremer.[84] (2) The TEP, which is based on one or an average of the CO stretching frequencies, is at best a qualitative measure for the Ni−Y bond strength as it is flawed in two ways: (i) The TEP and its computational equivalent, the CEP, are flawed by mode−mode coupling of the CO stretching modes with Ni−C stretching, Ni−C−O bending, and other vibrational modes. Mode coupling leads to CO stretching frequencies of L−Ni$(CO)_3$, which are contaminated by coupling frequencies of 20−200 $cm^{-1}$ and which therefore can no longer provide a reliable measure of the CO bond strength. (ii) There is no general relationship between the CO and the Ni−L stretching force constants (or frequencies). We find among the ligands investigated only one group of ligands, the halogenide anions (5 examples out of 181 Ni-complexes), for which, in line with Tolman's expectations, a quantitatively correct inverse relationship between CO and NiL stretching force constants can be derived. In all other cases, Ni−L stretching force constants scatter strongly for an increase in the CO force constants where inverse, no, or direct relationships can be. (3) Since TEP and CEP are of little use to describe Ni−L bonding, we have introduced a new metal−ligand electronic parameter (MLEP) in form of the local Ni−L stretching force constant $k^a$(NiY) where Y is that atom of the ligand directly bonded to the metal. Utilizing the local $k^a$ values of suitable reference molecules, the local stretching force constants $k^a$(NiY) are converted into relative bond strength orders (BSOs). Hence the new MLEP is discussed in terms of the BSO values, which provide a direct and quantitative measure of the intrinsic Ni−L bond strength. (4) By using $Ni(CO)_4$ as a suitable reference, one can differentiate between normal, strong, very strong, weak, and very weak NiY bonding. The differences in NiY bonding are caused by the interplay of essentially five different electronic effects: (i) $\sigma$-donation of the ligand, (ii) steric interactions of the ligand with the $Ni(CO)_3$ group, (iii) $\pi$−acceptor abilities of the ligand leading to delocalization of 3d(Ni) electrons, (iv) $\pi$-donor abilities of the ligand leading to delocalization L electrons into empty Ni orbitals, and (v) scalar relativistic effects of Y being a sixth period element reduce especially the $\sigma$-donor capacity of the ligand besides changing also $\pi$-acceptor and $\pi$-donor abilities. (5) Destabilizing steric interactions between L and $Ni(CO)_3$ group are directly determined by the MLEP and do not require a second parameter as in the case of the TEP (the cone angle of L). Low BSO values for a number of ligands such as triethyl, triphenyl, or triamino phosphines, amines, etc., can be directly related to steric effects. If needed, the local C−Ni−Y bending force constants provide the


DOI: 10.1021/acs.inorgchem.5b02711
Inorg. Chem. 2016, 55, 2332−2344

possibility of separating steric effects from other electronic interactions. (6) Amines, phosphines, arsines, stibines, and bismuthines (in each case 20 different of them leading to a total 100 ligands) have been investigated with the MLEP. The latter reveals the importance of $\pi$-back-donation from Ni into a low-lying pseudo-$\pi^*(PX_m)$ orbital for Ni−L bonding, which in this work was quantified with the help of second order perturbation theory leading to NBO delocalization energies. The variation in Ni−L bonding is large if $\pi$-back-donation plays an important role for the Ni−L bond strength. The average BSO value of the phosphines, arsines, stibines, amines, and bismuthines decreases as the $\sigma$-donor and $\pi$-acceptor abilities are reduced in this order. (7) Methylene leads to relatively strong Ni−L bonding according to the calculated MLEP value because a carbene has both $\pi$-acceptor and $\sigma$-donor capacity. The NiC bond strength is reduced in the way that the carbene is substituted by $\pi$-donors or herconjugative groups such as alkyl substituents. Arduengo carbenes have BSO values in a range from 0.57 to 0.67 where Ni−C bonding is strengthened with the tendency of forming a delocalized 6$\pi$-electronic system in the carbene ring. The Arduengo carbenes represent a group of ligands that have a reverse rather than inverse CO,NiY-relationship as shown in Figure 4. This shows the problem of using TEP parameters for the description of Arduengo carbene−metal bonding. (8) Cationic ligands lead to relatively large MLEP values provided steric factors do not play a role. A BSO value of 2.37 is found for the methylidyne cation $CH^+$ whereas the methyl cation has a BSO value of 0.72 because of the lack of any $\sigma$-donor ability. In the case of the t-butyl cation, NiC bonding is established by weak agostic interactions. The BSO values of anionic ligands vary in the range from 0.4 to 0.7. (9) Although we have shown that the results of a harmonic or anharmonically corrected quantum chemical description of the vibrational frequencies lead to similar BSO values, this work makes it desirable to verify MLEP values with the help of measured frequencies, which do not depend on any deficiencies of the quantum chemical method used. This should be possible in all those cases where the NiL stretching frequency can be detected in the normal infrared where its identification can be facilitated with the help of the vibrational frequencies calculated. However, many metal−ligand stretching frequencies appear in the far-infrared. They are only measurable with advanced spectroscopic methods such as terahertz spectroscopy or depolarized Raman scattering. Since these methods will become more and more available as there is need for them, this work underlines the need for equipment in chemical laboratories which makes far-infrared spectra available. (10) The BSO parameter describes the intrinsic strength of the ML bond and as such cannot be anticipated with the help of measured or calculated bond quantities referring to other properties of the ML bond. For example, there is no quantitative relationship between bond length and BSO. Also, the Wiberg index (measuring the bond multiplicity) of the NiL bond is not related to the corresponding BSO value and therefore does not provide a computationally less expensive tool to replace the BSO value.

This work has shown that for nickel−carbonyl complexes the TEP is of little use and should be replaced by the MLEP. Future work will focus on Au-complexes, where the TEP is known to fail.[44] Also, Ru-, Rh-, Re-, and Ir-complexes will be systematically investigated to provide MLEP values.

## ■ ASSOCIATED CONTENT

### Supporting Information

The Supporting Information is available free of charge on the ACS Publications website at DOI: 10.1021/acs.inorgchem.5b02711.

For calculated CO and NiY, bond lengths, local mode stretching force constants, frequencies, relative bond strength orders, and Cartesian coordinates of all optimized geometries (PDF)

## ■ AUTHOR INFORMATION


### Corresponding Author

*E-mail: dieter.cremer@gmail.com.


### Notes

The authors declare no competing financial interest.

## ■ ACKNOWLEDGMENTS

This work was financially supported by the National Science Foundation, Grants CHE 1464906 and CHE 1152357. We thank SMU for providing computational resources.

## ■ REFERENCES


(1) Tolman, C. A. *J. Am. Chem. Soc.* **1970**, *92*, 2953−2956.
(2) Tolman, C. A. *Chem. Rev.* **1977**, *77*, 313−348.
(3) Strohmeier, W.; Guttenberger, J. *Chem. Ber.* **1964**, *97*, 1871−1876.
(4) Strohmeier, W.; Müller, F. *Z. Naturforsch., B: J. Chem. Sci.* **1967**, *22B*, 451−452.
(5) Kraihanzel, C. S.; Cotton, F. A. *Inorg. Chem.* **1963**, *2*, 533−540.
(6) Cotton, F. A. *Inorg. Chem.* **1964**, *3*, 702−711.
(7) Crabtree, R. H. *The Organometallic Chemistry of the Transition Metals*; John Wiley & Sons: New York, 2009.
(8) Tolman, C. A. *Chem. Soc. Rev.* **1972**, *1*, 337−353.
(9) Horrocks, W. D., Jr.; Taylor, R. C. *Inorg. Chem.* **1963**, *2*, 723−727.
(10) Magee, T. A.; Matthews, C. N.; Wang, T. S.; Wotiz, J. *J. Am. Chem. Soc.* **1961**, *83*, 3200−3203.
(11) Bond, A. M.; Carr, S. W.; Colton, R. *Organometallics* **1984**, *3*, 541−548.
(12) Grim, S.; Wheatland, D.; McFarlane, W. *J. Am. Chem. Soc.* **1967**, *89*, 5573−5577.
(13) Alyea, E.; Ferguson, G.; Somogyvari, A. *Organometallics* **1983**, *2*, 668−674.
(14) Box, J. W.; Gray, G. M. *Magn. Reson. Chem.* **1986**, *24*, 527−533.
(15) Dalton, J.; Paul, I.; Smith, J. G.; Stone, F. A. *J. Chem. Soc. A* **1968**, 1195−1199.
(16) Brown, R.; Dobson, G. *Inorg. Chim. Acta* **1972**, *6*, 65−71.
(17) Woodard, S.; Angelici, R.; Dombek, B. *Inorg. Chem.* **1978**, *17*, 1634−1639.
(18) Angelici, R.; Malone, M. D. *Inorg. Chem.* **1967**, *6*, 1731−1736.
(19) Bancroft, M.; Dignard-Bailey, L.; Puddephatt, R. *Inorg. Chem.* **1986**, *25*, 3675−3680.
(20) Schulze, B.; Schubert, U. S. *Chem. Soc. Rev.* **2014**, *43*, 2522−2571.
(21) Check, C. T.; Jang, K. P.; Schwamb, C. B.; Wong, A. S.; Wang, M. H.; Scheidt, K. A. *Angew. Chem., Int. Ed.* **2015**, *54*, 4264−4268.
(22) Box, J. W.; Gray, G. M. *Inorg. Chem.* **1987**, *26*, 2774−2778.
(23) Petrov, A. R.; Derheim, A.; Oetzel, J.; Leibold, M.; Bruhn, C.; Scheerer, S.; Oßwald, S.; Winter, R. F.; Siemeling, U. *Inorg. Chem.* **2015**, *54*, 6657−6670.
(24) Darensbourg, D.; Nelson, H., III; Hyde, C. *Inorg. Chem.* **1974**, *13*, 2135−2145.
(25) Cunningham, D.; Goldschmidt, Z.; Gottlieb, H.; Hezroni-Langerman, D.; Howell, J. A. S.; Palin, M. G.; McArdle, P. *Inorg. Chem.* **1991**, *30*, 4683−4685.




DOI: 10.1021/acs.inorgchem.5b02711
*Inorg. Chem.* 2016, 55, 2332−2344

(26) Inoue, H.; Nakagome, T.; Kuroiwa, T.; Shirai, T.; Fluck, E. *Z. Naturforsch., B: J. Chem. Sci.* **1987**, *42B*, 573−578.
(27) Smith, R.; Baird, M. *Inorg. Chim. Acta* **1982**, *62*, 135−139.
(28) Howard, J.; Lovatt, J.; McArdle, P.; Cunningham, D.; Maimone, E.; Gottlieb, H.; Goldschmidt, Z. *Inorg. Chem. Commun.* **1998**, *1*, 118−120.
(29) Weinberger, D. S.; Lavallo, V. In *Handbook of Metathesis: Catalyst Development and Mechanism*; Grubbs, R. H., Wenzel, A. G., O'Leary, D. J., Khosravi, E., Eds.; Wiley-VCH Verlag GmbH: Berlin, 2015; pp 87−95.
(30) Hopkinson, M. N.; Richter, C.; Schedler, M.; Glorius, F. *Nature* **2014**, *510*, 485−496.
(31) Dröge, T.; Glorius, F. *Angew. Chem., Int. Ed.* **2010**, *49*, 6940−6952.
(32) Nelson, D. J.; Nolan, S. P. *Chem. Soc. Rev.* **2013**, *42*, 6723−6753.
(33) Sato, T.; Yoshioka, D.; Hirose, Y.; Oi, S. *J. Organomet. Chem.* **2014**, *753*, 20−26.
(34) Borguet, Y.; Zaragoza, G.; Demonceau, A.; Delaude, L. *Dalton Trans.* **2015**, *44*, 9744−9755.
(35) Otto, S.; Roodt, A. *Inorg. Chim. Acta* **2004**, *357*, 1−10.
(36) Serron, S.; Huang, J.; Nolan, S. *Organometallics* **1998**, *17*, 534−539.
(37) Roodt, A.; Otto, S.; Steyl, G. *Coord. Chem. Rev.* **2003**, *245*, 121−137.
(38) Fürstner, A.; Alcarazo, M.; Krause, H.; Lehmann, C. W. *J. Am. Chem. Soc.* **2007**, *129*, 12676−12677.
(39) Canac, Y.; Lepetit, C.; Abdalilah, M.; Duhayon, C.; Chauvin, R. *J. Am. Chem. Soc.* **2008**, *130*, 8406−8413.
(40) Valdes, H.; Poyatos, M.; Peris, E. *Inorg. Chem.* **2015**, *54*, 3654−3659.
(41) Tapu, D.; McCarty, Z.; Hutchinson, L.; Ghattas, C.; Chowdhury, M.; Salerno, J.; VanDerveer, D. *J. Organomet. Chem.* **2014**, *749*, 134−141.
(42) Wünsche, M. A.; Mehlmann, P.; Witteler, T.; Buß, F.; Rathmann, P.; Dielmann, F. *Angew. Chem., Int. Ed.* **2015**, *54*, 11857−11860.
(43) Valdes, H.; Poyatos, M.; Peris, E. *Organometallics* **2015**, *34*, 1725−1729.
(44) Ciancaleoni, G.; Scafuri, N.; Bistoni, G.; Macchioni, A.; Tarantelli, F.; Zuccaccia, D.; Belpassi, L. *Inorg. Chem.* **2014**, *53*, 9907−9916.
(45) Ciancaleoni, G.; Biasiolo, L.; Bistoni, G.; Macchioni, A.; Tarantelli, F.; Zuccaccia, D.; Belpassi, L. *Chem. - Eur. J.* **2015**, *21*, 2467−2473.
(46) Collado, A.; Patrick, S. R.; Gasperini, D.; Meiries, S.; Nolan, S. P. *Beilstein J. Org. Chem.* **2015**, *11*, 1809−1814.
(47) Kim, B.; Park, N.; Lee, S. M.; Kim, H. J.; Son, S. U. *Polym. Chem.* **2015**, *6*, 7363−7367.
(48) Perrin, L.; Clot, E.; Eisenstein, O.; Loch, J.; Crabtree, R. H. *Inorg. Chem.* **2001**, *40*, 5806−5811.
(49) Gusev, D. G. *Organometallics* **2009**, *28*, 763−770.
(50) Gusev, D. G. *Organometallics* **2009**, *28*, 6458−6461.
(51) Tonner, R.; Frenking, G. *Organometallics* **2009**, *28*, 3901−3905.
(52) Zobi, F. *Inorg. Chem.* **2009**, *48*, 10845−10855.
(53) Fianchini, M.; Cundari, T. R.; DeYonker, N. J.; Dias, H. V. R. *Dalton Trans.* **2009**, 2085−2087.
(54) Mathew, J.; Suresh, C. H. *Inorg. Chem.* **2010**, *49*, 4665−4669.
(55) Gusev, D. G. *Organometallics* **2009**, *28*, 763−770.
(56) Kalescky, R.; Kraka, E.; Cremer, D. *Inorg. Chem.* **2014**, *53*, 478−495.
(57) Zeinalipour-Yazdi, C. D.; Cooksy, A. L.; Efstathiou, A. M. *Surf. Sci.* **2008**, *602*, 1858−1862.
(58) Gillespie, A.; Pittard, K.; Cundari, T.; White, D. *IEJMD* **2002**, *1*, 242−251.
(59) Cooney, K. D.; Cundari, T. R.; Hoffman, N. W.; Pittard, K. A.; Temple, M. D.; Zhao, Y. *J. Am. Chem. Soc.* **2003**, *125*, 4318−4324.
(60) Fey, N.; Orpen, A. G.; Harvey, J. N. *Coord. Chem. Rev.* **2009**, *253*, 704−722.
(61) Fey, N. *Dalton Trans.* **2010**, *39*, 296−310.
(62) Kühl, O. *Coord. Chem. Rev.* **2005**, *249*, 693−704.
(63) Arduengo, A., III; Harlow, R.; Kline, M. *J. Am. Chem. Soc.* **1991**, *113*, 361−363.
(64) Arduengo, A. J. *Acc. Chem. Res.* **1999**, *32*, 913−921.
(65) Runyon, J. W.; Steinhof, O.; Dias, H. V. R.; Calabrese, J. C.; Marshall, W. J.; Arduengo, A. J. *Aust. J. Chem.* **2011**, *64*, 1165−1172.
(66) Arduengo, A. J.; Dolphin, J. S.; Gurau, G.; Marshall, W. J.; Nelson, J. C.; Petrov, V. A.; Runyon, J. W. *Angew. Chem., Int. Ed.* **2013**, *52*, 5110−5114.
(67) Nelson, D. J. *Eur. J. Inorg. Chem.* **2015**, *2015*, 2012−2027.
(68) Yang, B.-M.; Xiang, K.; Tu, Y.-Q.; Zhang, S.-H.; Yang, D.-T.; Wang, S.-H.; Zhang, F.-M. *Chem. Commun.* **2014**, *50*, 7163−7165.
(69) Jonek, M.; Diekmann, J.; Ganter, C. *Chem. - Eur. J.* **2015**, *21*, 15759−15768.
(70) Lever, A. *Inorg. Chem.* **1990**, *29*, 1271−1285.
(71) Lever, A. *Inorg. Chem.* **1991**, *30*, 1980−1985.
(72) Suresh, C.; Koga, N. *Inorg. Chem.* **2002**, *41*, 1573−1578.
(73) Giering, W.; Prock, A.; Fernandez, A. *Inorg. Chem.* **2003**, *42*, 8033−8037.
(74) Alyea, E.; Song, S. *Comments Inorg. Chem.* **1996**, *18*, 189−221.
(75) Coll, D. S.; Vidal, A. B.; Rodríguez, J. A.; Ocando-Mavárez, E.; Añez, R.; Sierraalta, A. *Inorg. Chim. Acta* **2015**, *436*, 163−168.
(76) Verlinden, K.; Buhl, H.; Frank, W.; Ganter, C. *Eur. J. Inorg. Chem.* **2015**, *2015*, 2416−2425.
(77) Shi, Q.; Thatcher, R. J.; Slattery, J.; Sauari, P. S.; Whitwood, A. C.; McGowan, P. C.; Douthwaite, R. E. *Chem. - Eur. J.* **2009**, *15*, 11346−11360.
(78) Valyaev, D. A.; Brousses, R.; Lugan, N.; Fernandez, I.; Sierra, M. A. *Chem. - Eur. J.* **2011**, *17*, 6602−6605.
(79) Uppal, B. S.; Booth, R. K.; Ali, N.; Lockwood, C.; Rice, C. R.; Elliott, P. I. P. *Dalton Trans.* **2011**, *40*, 7610−7616.
(80) Nelson, D. J.; Collado, A.; Manzini, S.; Meiries, S.; Slawin, A. M.; Cordes, D. B.; Nolan, S. P. *Organometallics* **2014**, *33*, 2048−2058.
(81) Donald, K. J.; Tawfik, M.; Buncher, B. *J. Phys. Chem. A* **2015**, *119*, 3780−3788.
(82) Flanigan, D. M.; Romanov-Michailidis, F.; White, N. A.; Rovis, T. *Chem. Rev.* **2015**, *115*, 9307−9387.
(83) van Weerdenburg, B. J.; Eshuis, N.; Tessari, M.; Rutjes, F. P.; Feiters, M. C. *Dalton Trans.* **2015**, *44*, 15387−15390.
(84) Konkoli, Z.; Cremer, D. *Int. J. Quantum Chem.* **1998**, *67*, 1−9.
(85) Zou, W.; Kalescky, R.; Kraka, E.; Cremer, D. *J. Chem. Phys.* **2012**, *137*, 084114−084114.
(86) Zou, W.; Kalescky, R.; Kraka, E.; Cremer, D. *J. Chem. Phys.* **2012**, *137*, 084114.
(87) Zou, W.; Cremer, D. *Theor. Chem. Acc.* **2014**, *133*, 1451.
(88) Wilson, E. B.; Decius, J. C.; Cross, P. C. *Molecular Vibrations. The Theory of Infrared and Raman Vibrational Spectra*; McGraw-Hill: New York, 1955.
(89) Kalescky, R.; Zou, W.; Kraka, E.; Cremer, D. *Chem. Phys. Lett.* **2012**, *554*, 243−247.
(90) Kalescky, R.; Kraka, E.; Cremer, D. *Mol. Phys.* **2013**, *111*, 1497−1510.
(91) Cremer, D.; Larsson, J. A.; Kraka, E. In *Theoretical and Computational Chemistry, Vol. 5, Theoretical Organic Chemistry*; Parkanyi, C., Ed.; Elsevier: Amsterdam, 1998; pp 259−327.
(92) Konkoli, Z.; Cremer, D.; Kraka, E. *J. Phys. Chem. A* **1997**, *101*, 1742−1757.
(93) Zhao, Y.; Truhlar, D. *Theor. Chem. Acc.* **2008**, *120*, 215.
(94) Becke, A. D. *J. Chem. Phys.* **1993**, *98*, 5648−5652.
(95) Chai, J.-D.; Head-Gordon, M. *Phys. Chem. Chem. Phys.* **2008**, *10*, 6615−6620.
(96) Chai, J.-D.; Head-Gordon, M. *J. Chem. Phys.* **2008**, *128*, 084106.
(97) Dunning, T. *J. Chem. Phys.* **1989**, *90*, 1007−1023.
(98) Woon, D.; Dunning, T. *J. Chem. Phys.* **1993**, *98*, 1358−1371.
(99) Wilson, A.; Woon, D.; Peterson, K.; Dunning, T. *J. Chem. Phys.* **1999**, *110*, 7667−7676.
(100) Peterson, K. A. *J. Chem. Phys.* **2003**, *119*, 11099.
(101) Peterson, K. A.; Figgen, D.; Goll, E.; Stoll, H.; Dolg, M. *J. Chem. Phys.* **2003**, *119*, 11113.


DOI: 10.1021/acs.inorgchem.5b02711
*Inorg. Chem.* 2016, 55, 2332−2344

(102) Gräfenstein, J.; Cremer, D. *J. Chem. Phys.* **2007**, *127*, 164113.
(103) Freindorf, M.; Kraka, E.; Cremer, D. *Int. J. Quantum Chem.* **2012**, *112*, 3174−3187.
(104) Kraka, E.; Cremer, D. *ChemPhysChem* **2009**, *10*, 686−698.
(105) Kalescky, R.; Zou, W.; Kraka, E.; Cremer, D. *J. Phys. Chem. A* **2014**, *118*, 1948−1963.
(106) Kalescky, R.; Kraka, E.; Cremer, D. *J. Phys. Chem. A* **2013**, *117*, 8981−8995.
(107) Badger, R. M. *J. Chem. Phys.* **1934**, *2*, 128−131.
(108) Kraka, E.; Larsson, J. A.; Cremer, D. In *Computational Spectroscopy: Methods, Experiments and Applications*; Grunenberg, J., Ed.; John Wiley & Sons: New York, 2010; pp 105−149.
(109) Wiberg, K. *Tetrahedron* **1968**, *24*, 1083−1096.
(110) Mayer, I. *J. Comput. Chem.* **2007**, *28*, 204−221.
(111) Barone, V. *J. Chem. Phys.* **2005**, *122*, 014108.
(112) Kalescky, R.; Kraka, E.; Cremer, D. *Int. J. Quantum Chem.* **2014**, *114*, 1060−1072.
(113) Reed, A.; Curtiss, L.; Weinhold, F. *Chem. Rev.* **1988**, *88*, 899.
(114) Weinhold, F.; Landis, C. R. *Discovering Chemistry with Natural Bond Orbitals*; Cambridge University Press: Cambridge, U.K., 2003.
(115) Glendening, E. D.; Landis, C. R.; Weinhold, F. *J. Comput. Chem.* **2013**, *34*, 1429−1437.
(116) Porterfield, W. W. *Inorganic Chemistry, A Unified Approach*; Academic Press: San Diego, CA, 1993.
(117) Anderson, S. *Introduction to Inorganic Chemistry*; University Science Books: Sausalito, CA, 2004.
(118) Kraka, E.; Zou, W.; Filatov, M.; Grafenstein, J.; Izotov, D.; Gauss, J.; He, Y.; Wu, A.; Polo, V.; Olsson, L.; Konkoli, Z.; He, Z.; Cremer, D. *COLOGNE2015*; Southern Methodist University: Dallas, TX, 2015.
(119) Zou, W.; Cremer, D. *Local Mode Programm*; Southern Methodist University: Dallas, TX, 2015.
(120) Frisch, M.; Trucks, G.; Schlegel, H.; Scuseria, G.; Robb, M. A.; Cheeseman, J. R.; Scalmani, G.; Barone, V.; Mennucci, B.; Petersson, G.; Nakatsuji, H.; Caricato, M.; Li, X.; Hratchian, H.; Izmaylov, A.; Bloino, J.; Zheng, G.; Sonnenberg, J.; Hada, M.; Ehara, M.; Toyota, K.; Fukuda, R.; Hasegawa, J.; Ishida, M.; Nakajima, T.; Honda, Y.; Kitao, O.; Nakai, H.; Vreven, T.; Montgomery, J. A., Jr.; Peralta, J. E.; Ogliaro, F.; Bearpark, M.; Heyd, J.; Brothers, E.; Kudin, K.; Staroverov, V.; Kobayashi, R.; Normand, J.; Raghavachari, K.; Rendell, A.; Burant, J.; Iyengar, S.; Tomasi, J.; Cossi, M.; Rega, N.; Millam, J.; Klene, M.; Knox, J.; Cross, J.; Bakken, V.; Adamo, C.; Jaramillo, J.; Gomperts, R.; Stratmann, R.; Yazyev, O.; Austin, A.; Cammi, R.; Pomelli, C.; Ochterski, J.; Martin, R.; Morokuma, K.; Zakrzewski, V.; Voth, G.; Salvador, P.; Dannenberg, J.; Dapprich, S.; Daniels, A.; Farkas, O.; Foresman, J.; Ortiz, J.; Cioslowski, J.; Fox, D. *Gaussian 09 Revision D.1*; Gaussian Inc.: Wallingford, CT, 2010.
(121) McIntosh, A. I.; Yang, B.; Goldup, S. M.; Watkinson, M.; Donnan, R. S. *Chem. Soc. Rev.* **2012**, *41*, 2072−2082.
(122) Mantsch, H. H.; Naumann, D. *J. Mol. Struct.* **2010**, *964*, 1−4.
(123) Parrott, E. P. J.; Sun, Y.; Pickwell-MacPherson, E. *J. Mol. Struct.* **2011**, *1006*, 66−76.
(124) Majhi, P. K.; Serin, S. C.; Schnakenburg, G.; Gates, D. P.; Streubel, R. *Eur. J. Inorg. Chem.* **2014**, *2014*, 4975−4983.
(125) Soleilhavoup, M.; Bertrand, G. *Acc. Chem. Res.* **2015**, *48*, 256−266.
(126) Uzelac, M.; Hernán-Gómez, A.; Armstrong, D. R.; Kennedy, A. R.; Hevia, E. *Chem. Sci.* **2015**, *6*, 5719−5728.

## ■ NOTE ADDED AFTER ISSUE PUBLICATION

Figures 9−13 were incorrect in the version published on February 22, 2016. The revised version was published on the Web on March 23, 2016. An Addition & Correction was published in volume 55, issue 7.



DOI: 10.1021/acs.inorgchem.5b02711
*Inorg. Chem.* 2016, 55, 2332−2344